pISSN 2384-1095
eISSN 2384-1109

iMRI 2021;25:118-128

https://doi.org/10.13104/imri.2021.25.2.118

iMRI
Investigative Magnetic Resonance Imaging

Benign versus Malignant Soft-Tissue Tumors: Differentiation with 3T Magnetic Resonance Image Textural Analysis Including Diffusion-Weighted Imaging

Youngjun Lee[1,2], Won-Hee Jee[1,3], Yoon Sub Whang[4], Chan Kwon Jung[5], Yang-Guk Chung[6], So-Yeon Lee[1]

Departments of [1]Radiology, [5]Pathology, and [6]Orthopedic Surgery, Seoul St. Mary's Hospital, College of Medicine, The Catholic University of Korea, Seoul, Korea
[4]Department of Radiology, Myongji St. Mary's Hospital, Seoul, Korea
[2]Department of Radiology, Uijeongbu St. Mary's Hospital, College of Medicine, The Catholic University of Korea, Kyunggido, Korea
[3]Department of Radiology, Heemyoung Medical Center, Seoul, Korea

Original Article

Received: March 9, 2021
Revised: April 25, 2021
Accepted: April 26, 2021

Correspondence to:
So-Yeon Lee, M.D.
Department of Radiology, Seoul St. Mary's Hospital, College of Medicine, The Catholic University of Korea, 222 Banpo-daero, Seocho-gu, Seoul 06591, Korea.
Tel. +82-2-2258-6743
Fax. +82-2-599-6771
E-mail: capella27@gmail.com

Purpose: To investigate the value of MR textural analysis, including use of diffusion-weighted imaging (DWI) to differentiate malignant from benign soft-tissue tumors on 3T MRI.

Materials and Methods: We enrolled 69 patients (25 men, 44 women, ages 18 to 84 years) with pathologically confirmed soft-tissue tumors (29 benign, 40 malignant) who underwent pre-treatment 3T-MRI. We calculated MR texture, including mean, standard deviation (SD), skewness, kurtosis, mean of positive pixels (MPP), and entropy, according to different spatial-scale factors (SSF, 0, 2, 4, 6) on axial T1- and T2-weighted images (T1WI, T2WI), contrast-enhanced T1WI (CE-T1WI), high b-value DWI (800 sec/mm^2), and apparent diffusion coefficient (ADC) map. We used the Mann-Whitney U test, logistic regression, and area under the receiver operating characteristic curve (AUC) for statistical analysis.

Results: Malignant soft-tissue tumors had significantly lower mean values of DWI, ADC, T2WI and CE-T1WI, MPP of ADC, and CE-T1WI, but significantly higher kurtosis of DWI, T1WI, and CE-T1WI, and entropy of DWI, ADC, and T2WI than did benign tumors ($P < 0.050$). In multivariate logistic regression, the mean ADC value (SSF, 6) and kurtosis of CE-T1WI (SSF, 4) were independently associated with malignancy ($P \leq 0.009$). A multivariate model of MR features worked well for diagnosis of malignant soft-tissue tumors (AUC, 0.909).

Conclusion: Accurate diagnosis could be obtained using MR textural analysis with DWI and CE-T1WI in differentiating benign from malignant soft-tissue tumors.

Keywords: Magnetic resonance imaging; Diffusion; Texture analysis; Sarcoma; Neoplasm

INTRODUCTION

Soft-tissue tumors are a group of diseases consisting of various neoplasms. The World Health Organization (WHO) classifies soft-tissue tumors into benign, intermediate, and malignant tumors (1). Diagnosis of sarcoma is important, because its prognosis and treatment are different from those of benign lesions. Malignancy is traditionally treated with wide excision and radiotherapy; however, limb-conserving surgery or chemotherapy may be considered in some cases. An operation based on an inadequate preoperative plan, a so-called 'unplanned' or 'whoops' surgery, results in an inappropriate range of resection and increased local tumor recurrence unless followed by subsequent management. Imaging before surgery not only assesses the possibility of malignancy, but also helps in surgical planning by evaluating the relationship between the tumor and surrounding tissues (2-4).

Magnetic resonance imaging (MRI) is currently considered to be the standard diagnostic tool for evaluating soft-tissue mass (5). It is often challenging to distinguish benign from malignant soft-tissue tumors on MRI, except for a few types of tumors, such as lipoma and peripheral nerve sheath tumors (4). In general, heterogeneous signal intensity on T2-weighted imaging (T2WI), deep location, and larger size (> 5 cm) are suggestive of malignant soft-tissue tumors. Systematic combination of these findings showed a sensitivity of 64%, specificity of 85%, and accuracy of 77% (6). Homogeneous contrast-enhancement patterns of soft-tissue tumors were highly specific for benignity, and inhomogeneous contrast enhancement was moderately specific for malignancy on MRI with a sensitivity of 88.7% and a specificity of 59.7% (7). Diagnosis using standard MRI has been limited by a significant overlap of MRI findings. To overcome this limitation, additional techniques have been used, including diffusion-weighted imaging (DWI) and dynamic enhancement study (2, 3, 8, 9). Malignant tumors show high signal intensity on DWI with a high b value and a low apparent diffusion coefficient (ADC) in general. According to a previous study (8), malignant soft-tissue tumors had lower ADC values than did benign soft-tissue tumors: 759 ± 385 vs. 1188 ± 423 μm^2/sec minimum ADC value and 941 ± 440 vs. 1310 ± 440 μm^2/sec average ADC value. The addition of DWI to conventional MRI resulted in better diagnoses; sensitivity, specificity, and accuracy were 96%, 72%, and 85% on standard MRI alone and 97%, 90%, and 94% on standard MRI with DWI, respectively (8). For dynamic contrast-enhanced MRI (CE-MRI), parameters (K^{trans}, K_{ep}, V_e, iAUC, and time-concentration curve plots) were significantly different between benign and malignant tumors (9).

Quantitative analysis of MR images has been attempted in various musculoskeletal disorders (2, 8, 10-15), because it can provide additional information about images that are not found in conventional visual evaluations. Textural analysis of medical imaging is an emerging technique that provides information on intratumoral heterogeneity, which reflects cell density, necrosis, hemorrhage, or myxoid change (11, 16). This is not a visual assessment but a mathematical model that allows evaluation of gray-level intensity, position of pixels, arrangement, and interrelations among voxel intensities. According to recent articles, textural analysis of T2WI and T1-weighted images (T1WI) is useful in distinguishing malignant from benign soft-tissue tumors (11, 17, 18). As far as we know, the usefulness of textural analysis of DWI and gadolinium-enhancement studies on soft-tissue tumors has not been fully examined. Given previous findings that CE-MRI and DWI help diagnose malignant soft-tissue tumors, we estimate that textural analysis using these imaging techniques will also help to diagnose malignant soft-tissue tumors (2, 3, 7-9). Thus, our purpose in this study is to introduce the potential of MRI textural analysis, including DWI and CE-MRI, in differentiating benign from malignant tumors.

MATERIALS AND METHODS

Patient Population

This study was approved by our Institutional Review Board (IRB) and complied with the Health Insurance Portability and Accountability Act (HIPAA) guidelines. The requirement for informed consent was waived for this retrospective study by the IRB.

Between January 2014 and February 2019, there were 81 consecutive patients who met the inclusion criteria. These were patients who had had:

(1) MRI prior to treatment or biopsy of soft-tissue mass;
(2) MRI scans including DWI and gadolinium-enhancement study; and
(3) histopathologically confirmed tumors.

Exclusion criteria were:

(1) suboptimal image quality (n = 1);
(2) small lesions (less than 1 cm) (n =5);
(3) pathologic confirmation only by biopsy (n = 2); and

(4) technical error while loading images into software or extracting texture features using software (n = 4).

After applying the above standard selection, we excluded 12 lesions, leaving 69 for inclusion in this study (Fig. 1).

MR Imaging Protocols

All 69 patients in the study group were imaged using the 3.0T Magnetom Verio (Siemens, Erlangen, Germany) with various surface coils depending on the anatomic location of the tumor. Standard MRI protocol including axial T1WI, T2WI, contrast-enhanced T1WI (CE-T1WI), and at least one longitudinal image and fat-suppressed T2WI were obtained.

DWI was obtained prior to the contrast material administration by using a single-shot spin-echo echo-planar imaging pulse sequence prototype. A parallel imaging technique using GRAPPA (GeneRalized Autocalibrating Partially Parallel Acquisitions) was combined with an acceleration factor of 2. The echo-planar imaging factor was 56, and sensitizing diffusion gradients were applied sequentially in the *x*, *y*, and *z* directions with b values of 0 and 800 sec/mm^2 (8, 19). Pixel-based ADC maps were created by means of mono-exponential calculation from DWI with b values of 0 and 800 sec/mm^2 using a commercial software and workstation (Leonardo MR Workplace; Siemens Medical Solution, Erlangen, Germany) (8). Other MR parameters are presented in Table 1.

MR Image Analysis

We used a commercially available software called TexRAD (http://www.texrad.com, part of Feedback Plc, Cambridge, UK), which is based on a filtration-histogram method, for textural analysis (4, 12). One experienced radiologist (W.H.J., with 20 years of experience in musculoskeletal radiology) selected one axial plane on which to conduct the analysis. To reflect the characteristics of the entire tumor in one plane, the plane with the largest view of solid tumor portions (except for a hematoma or necrosis) was selected. When there were multiple such planes, one that contained areas of heterogeneity or good contrast enhancement was selected. The same radiologist (W.H.J.) manually drew the region of interest (ROI) in the selected plane (Fig. 2). After careful review of conventional images, ROIs were drawn in one area as large as possible (except for hematomas and necrosis). Because peritumoral tissue or partial volume artifacts might have been included, the peripheral border of tumors was avoided. After drawing the ROI on one sequence, the radiologist copied it, pasted it into the same planes of other sequences, and checked that the attached ROI did not include hematomas, necrosis, or the peripheral border of the tumor on each sequence. The radiologist repeated this three times to select the most appropriate ROI.

We calculated six textural features based on first-order statistics of the gray-level intensity histogram from raw images and filtered images using the Laplacian of Gaussian filter with four different spatial-scale factors (SSF) of 0, 2, 4, and 6 (12): mean (average of pixel value), standard

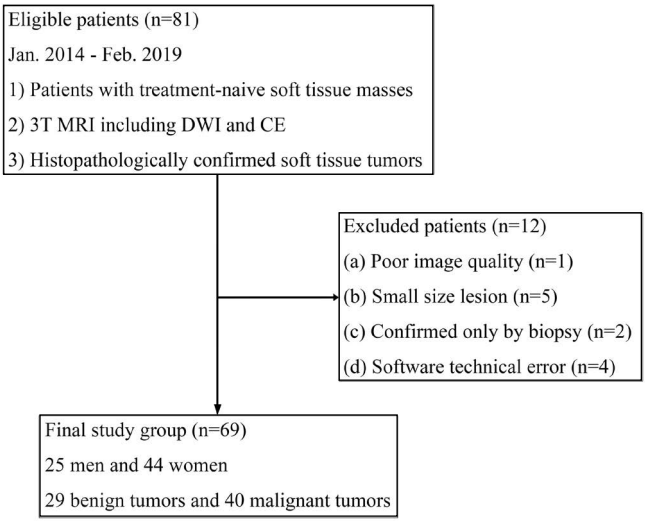

Fig. 1. Patient enrollment diagram.

Table 1. MR Parameters

Parameters	Conventional imaging	DWI
Field of view	80-220 mm	80-220 mm
Matrix size	512 × 256	64 × 45 - 120 × 128
TR (ms)/TE (ms)	T1WI, CE-T1WI: 680-870/11-21 T2WI: 4000-5600/63-83	5000-8700/71-85
Fat suppression	Chemical shift selective	Chemical shift selective
Section thickness	2-5 mm	2-5 mm
Intersection gap	No	No
Turbo factor or EPI factor	T1WI: 3 T2WI: 13	56
Number of excitation	1	3-5

CE-T1WI = contrast-enhanced T1-weighted image; DWI = diffusion-weighted image; EPI = echo-planar imaging; T1WI = T1-weighted image; T2WI = T2-weighted image

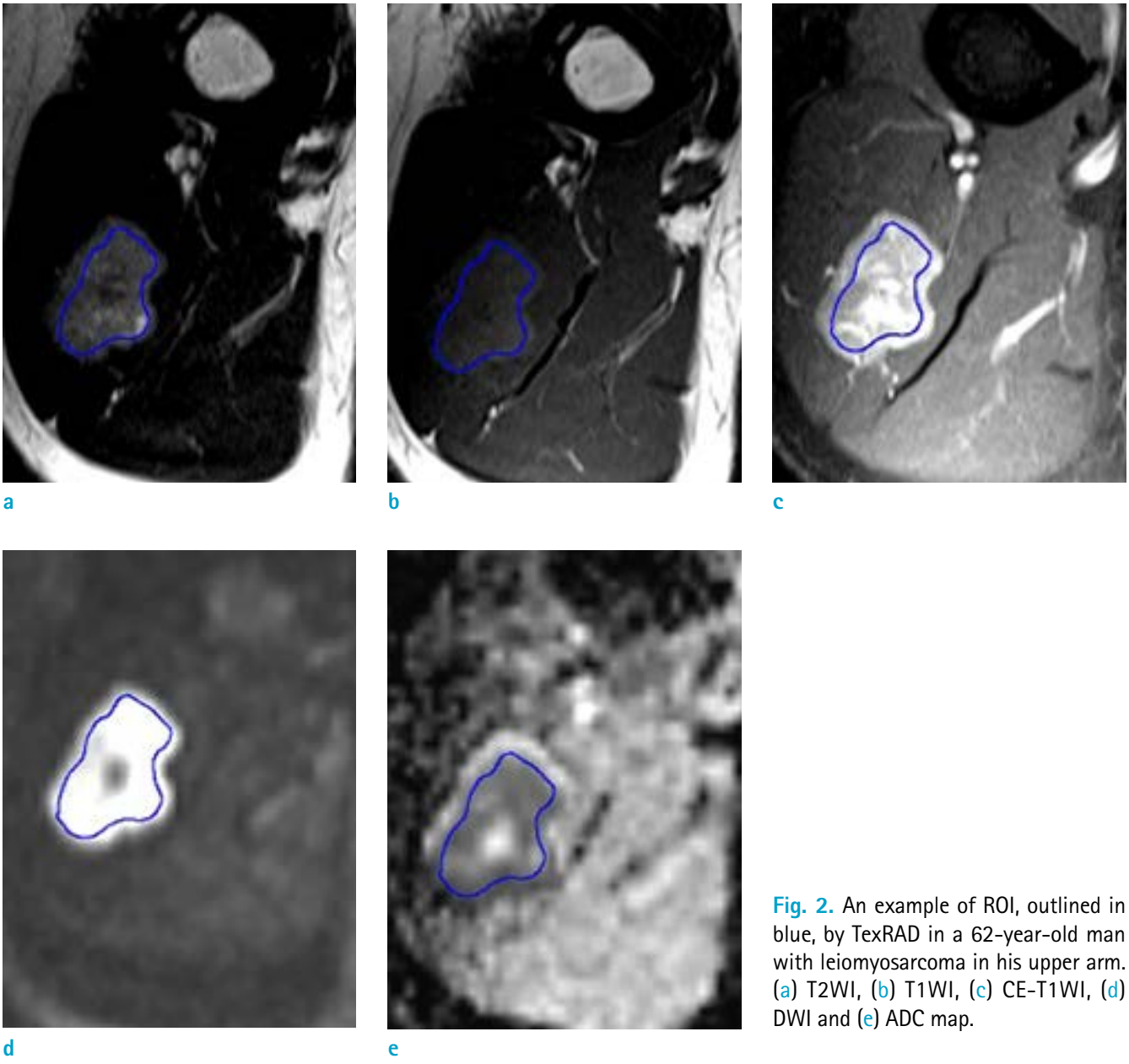

Fig. 2. An example of ROI, outlined in blue, by TexRAD in a 62-year-old man with leiomyosarcoma in his upper arm. (a) T2WI, (b) T1WI, (c) CE-T1WI, (d) DWI and (e) ADC map.

deviation (SD, degree of variation of intensity value), entropy (irregularity of gray-level distribution), mean of positive pixels (MPP, pixels with values greater than 0), skewness (asymmetry of a distribution), and kurtosis (degree of peakedness of a distribution). An SSF of 2 (SSF 2) enhanced a fine texture with a radius of 2 mm, an SSF of 4 (SSF 4) enhanced a medium texture with a radius of 4 mm, and an SSF of 6 (SSF 6) enhanced a coarse texture with a radius of 6 mm (20, 21) (Fig. 3). To reduce the signal difference between cases, we normalized parameters potentially affected by differences in gain factors including mean, SD, and MPP on T1WI, T2WI, and CE-T1WI by dividing them by the signal intensity of the skeletal muscle of each patient and at each filter SSF value (8, 12). Obtained features are summurized in Table 2. We measured tumor size by manually drawn ROI on T2WI within the largest tumor image on a picture archiving and communication system (PACS).

Statistical Analysis

We compared age and tumor size between benign

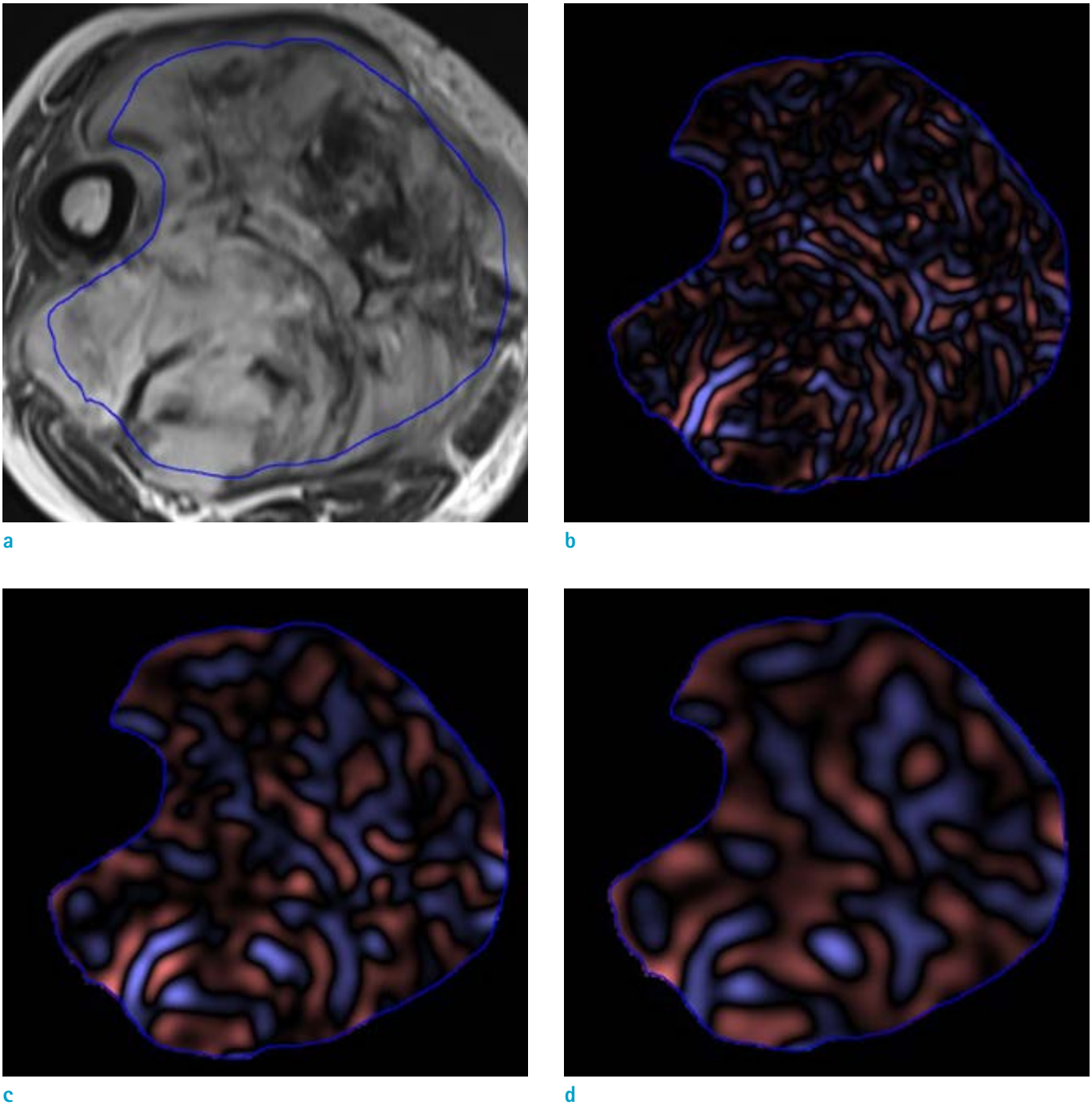

Fig. 3. An example of textural analysis done on T2WI of undifferentiated sarcoma in an 81-year-old woman. The tumor was manually delineated on T2WI (a, unfiltered image). Textural analysis was done within a region of interest after filtration by using SSFs of 2 (b, fine-texture features), 4 (c, medium-texture features), and 6 (d, coarse-texture features).

and malignant groups by a Mann-Whitney U test, and proportion of gender between the two groups by a chi-squared test. We did univariate analysis using a Mann-Whitney U test to compare MR texture parameters between the benign and malignant groups, and multivariate analysis after top-five MR feature selection by minimum redundancy maximum relevance (mRMR) decorrelation methods (22). We obtained the receiver operating characteristic curve with areas under the curve (AUC) for each parameter and multivariate model. We calculated the optimal cut-off value

Table 2. MR Texture Analysis Parameters

MR sequence	T1WI, T2WI, CE-T1WI, DWI, ADC	
Filtration using Laplacian of Gaussian filter	SSF 0	Unfiltered image
	SSF 2	Filtered image enhanced a fine-texture with radius of 2 mm
	SSF 4	Filtered image enhanced a medium-texture with radius of 4 mm
	SSF 6	Filtered image enhanced a coarse-texture with radius of 6 mm
First-order statistics of the gray-level intensity histogram	Mean	Average of pixel value
	SD	Degree of variation of intensity value
	Entropy	Irregularity of gray-level distribution
	MPP	Pixels with values greater than 0
	Skewness	Asymmetry of a distribution
	Kurtosis	Degree of peakedness of a distribution

ADC = apparent diffusion coefficient; CE-T1WI = contrast-enhanced T1-weighted image; DWI = diffusion-weighted image; MPP = mean of positive pixel; SD = standard deviation; SSF = spatial scale factors; T1WI = T1-weighted image; T2WI = T2-weighted image

All images acquired from each MR sequence are filtrated with value of SSF 2, 4, and 6. After filtration, 6 texture features were extracted from each filtered image (SSF 2, 4, 6), and raw image (SSF 0). Finally, 120 texture features were obtained.

using the Youden index (23) and compared AUCs with each other by DeLong's methods (24).

We considered a $P < 0.05$ as indicating a statistically significant difference in all tests. We did all statistical analyses using commercial software: SPSS, version 20, SPSS, Chicago, III; R.3.3.1 package pwr, The R Project for Statistical Computing, https://www.r-project.org; and Medcalc version 19.2.6.

RESULTS

Study Population

There were 69 patients with a mean age of 53 years (range, 18-84 years) and with 29 benign and 40 malignant tumors in the final study group. The benign soft-tissue tumor group included 8 male patients and 21 female patients; the malignant soft-tissue group included 17 male patients and 23 female patients. The median age of the benign soft-tissue tumor group was 47 years; that of the malignant soft-tissue tumor group was 57 years. There was no significant difference in gender ($P = 0.207$) or age ($P = 0.102$) between the two groups (Table 3). The tumors of the malignant group were significantly larger than were those of the benign group ($P < 0.001$); 1149.3 cm^2 [interquartile range (IQR), 318.6-3305.8 cm^2] vs. 206.3 cm^2 (IQR, 107.5-579.3 cm^2).

MR Textural Analysis

We extracted a total of 120 MR textural features. There were 69 significantly different features between the benign and malignant groups ($P \leq 0.049$, Table 4). We calculated the AUCs in each parameter; the parameters in which the AUC was statistically significant are listed in Tables 5 and 6. There were no significant differences of AUCs between sequences ($P > 0.050$). The mean ADC (SSF 6) showed the highest AUC, which was 0.852, followed by the mean ADC (SSF 4), which showed an AUC of 0.846.

The features selected from mRMR were as follows: mean ADC (SSF 6), mean ADC (SSF 4), entropy on DWI (SSF 2), kurtosis on DWI (SSF 2), and kurtosis on CE-T1WI (SSF 4). Multiple logistic regression after adjustment of tumor size revealed an independent association between mean ADC (SSF 6), kurtosis on CE-T1WI (SSF 4), and malignancy ($P < 0.001$). For mean ADC (SSF 6), sensitivity and specificity using optimal threshold levels of ≤ 353.15 were 85% (95% CI, 70.2-94.3%) and 82.8% (64.2-94.2%), respectively. For kurtosis on CE-T1WI (SSF 4), sensitivity and specificity using an optimal threshold level of > 0.43 were 85% (95% CI, 70.2-94.3%) and 68.97% (49.2-84.7%), respectively.

The AUC for the model of selected MR features for diagnosis of malignancy was 0.909 (95% CI 0.815-0.965) with a sensitivity of 95% and a specificity of 75.86%. The AUC for the combined model of selected MR and clinical features including age, sex, and tumor size for diagnosis of malignancy was 0.926 (95% CI 0.837-0.975) with a

Table 3. Summary of Clinical and Histopathologic Features

	Benign group (n = 29)	Malignant group (n = 40)	P value
Median age (years)[a]	47 (33-62 years)	57 (46-69 years)	0.102
Gender[b]	8:21	17:23	0.207
Pathologic result[c]	Schwannoma (8) Fibromatosis (5) Hemangioma (3) Tenosynovial giant cell tumor (3) Angiomyolipoma (3) Nodular fasciitis (2) Benign spindle cell neoplasm (1) Glomus tumor (1) Neurofibroma (1) Angiofibroma (1)	Undifferentiated sarcoma (10) Myxofibrosarcoma (5) Lymphoma (5) Synovial sarcoma (4) Malignant peripheral nerve sheath tumor (3) Myxoid liposarcoma (3) Epitheloid hemangioendothelioma (2) Alveolar rhabdomyosarcoma (1) Dedifferentiated liposarcoma (1) Malignant melanoma (1) Angiosarcoma (1) Myeloid sarcoma (1) Extraskeletal mesenchymal chondrosarcoma (1) Leiomyosarcoma (1) Malignant solitary fibrous tumor (1)	n/a

[a]Data are expressed as median (inter-quartile range) and were analyzed by Mann-Whitney U test.
[b]Data are expressed as male:female and were analyzed by chi-square test.
[c]Numbers in the parenthesis are numbers of cases.

sensitivity of 90% and a specificity of 72.41%. There was no significant difference between AUCs of mean ADC (SSF 6), multivariate model of MR features, or a combined model of MR and clinical features. The AUC of kurtosis on CE (SSF 4) was significantly lower than was the AUC of mean ADC (SSF 6), the multivariate model from MR features, or the combined model of MR and clinical features (Fig. 4).

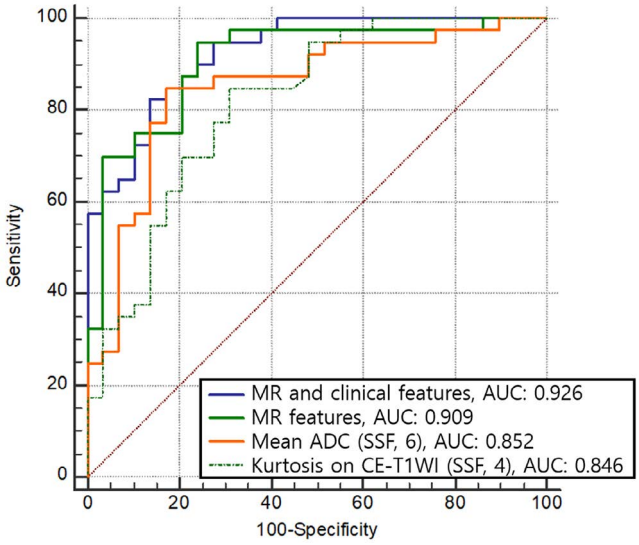

Fig. 4. The receiver operating characteristic curves for MR and clinical features for differentiating benign and malignant soft-tissue tumors.

DISCUSSION

Our preliminary analysis revealed that MRI-based textural analysis using DWI and CE-MRI allowed accurate diagnosis of malignant soft-tissue tumors. These preliminary results must be interpreted with caution until they have been validated by use of an independent dataset. However, our study newly demonstrated the usefulness of textural analysis of DWI and CE-T1WI for differentiating benign and malignant soft-tissue tumors. In addition, we newly demonstrated that mean ADC on a 6-mm coarse filter was an independent factor that strongly suggested malignancy with a single MR feature. The diagnostic performance of mean ADC (SSF 6) was comparable to that of a combined model of MR and clinical features. There has been no research comparing diagnostic performance in terms of different SSFs in soft-tissue tumors.

Our study revealed diagnostic accuracy comparable to that of recent studies in which standard MRI including T1WI and T2WI were used for textural analysis in diagnosing malignant soft-tissue tumors (17, 18). In a previous study (18) with 1.5T MRI of 91 soft-tissue masses, AUC using radiomics signature after feature reduction from

Table 4. Comparison of MR Texture Parameters between Benign and Malignant Soft Tissue Tumors (P values)

	SSF	T2WI	T1WI	CE-T1WI	DWI	ADC
Mean	0	0.929	0.770	0.088	0.015[a]	0.007[a]
	2	0.002[a]	0.174	<0.001[a]	0.002[a]	<0.001[a]
	4	0.001[a]	0.461	<0.001[a]	0.005[a]	<0.001[a]
	6	0.001[a]	0.469	<0.001[a]	0.049[a]	<0.001[a]
SD	0	0.788	0.611	0.774	0.010[a]	0.004[a]
	2	0.164	0.124	0.024[a]	0.803	0.798
	4	0.618	0.195	0.125	0.033[a]	0.031[a]
	6	0.919	0.340	0.832	0.001[a]	0.013[a]
MPP	0	0.929	0.770	0.088	0.015[a]	0.007[a]
	2	0.008[a]	0.071	0.001[a]	0.152	0.093
	4	0.017[a]	0.166	<0.001[a]	0.440	0.003[a]
	6	0.019[a]	0.140	<0.001[a]	0.852	0.003[a]
Skewness	0	0.001[a]	0.696	0.918	0.822	<0.001[a]
	2	0.112	0.581	0.111	0.331	0.349
	4	0.990	0.696	0.243	0.135	0.035[a]
	6	0.458	0.150	0.012[a]	0.020[a]	0.012[a]
Kurtosis	0	0.623	0.012[a]	0.114	0.008[a]	0.001[a]
	2	0.002[a]	0.001[a]	<0.001[a]	<0.001[a]	0.001[a]
	4	0.013[a]	0.001[a]	<0.001[a]	<0.001[a]	0.017[a]
	6	0.001[a]	0.001[a]	0.001[a]	0.002[a]	0.009[a]
Entropy	0	0.001[a]	0.036[a]	0.090[a]	<0.001[a]	<0.001[a]
	2	<0.001[a]	0.127	0.217	<0.001[a]	<0.001[a]
	4	<0.001[a]	0.108	0.096	<0.001[a]	<0.001[a]
	6	<0.001[a]	0.078	0.017	<0.001[a]	<0.001[a]

ADC = apparent diffusion coefficient; CE-T1WI = contrast-enhanced T1-weighted image; DWI = diffusion-weighted image; MPP = mean positive pixel; SD = standard deviation; SSF = special scale factor; T1WI = T1-weighted image; T2WI = T2-weighted image

Values are P-values obtained by Mann-Whitney U test for differentiation of benign and malignant soft tissue tumors.

[a]Values are statistically significant.

396 features based on T1WI and T2WI was 0.86. In another study (17) with machine learning for radiomics features, AUC was 0.81 to 1.00 in the training cohort with 3.0 T MRI of 69 soft-tissue lesions. In that study, 1132 features were extracted, and various feature-reduction methods were applied. Our study showed comparable accuracy using first-order MR parameters from CE-T1WI and DWI. There are thousands of parameters used in textural analysis. A previous study (18) used a higher-order parameter called radiomics, whereas our study used a first-order parameter known as histogram analysis. Recent studies showed that features in higher-order radiomics showed much redundancy (13, 14, 25), which is probably why our study with only a few features achieved accuracy similar to that of prior studies.

DWI with an ADC map is quantitative imaging, which is affected relatively little by differences in gain factors according to patient and MR scanners. Most parameters derived from ADC showed significant differences between benign and malignant soft-tissue tumors in this study. Like our results, first-order-based ADC parameters in 19 patients with 1.5 T MRI were significantly different between intermediate and high-grade sarcoma (15). Previous research on myxoid soft-tissue tumors reported a significant

Table 5. Diagnostic Performance of MR Texture Parameters from T2WI, T1WI and CE-T1WI for Differentiating Benign and Malignant Soft Tissue Tumors

Sequence	Texture parameter	SSF	AUC	Standard error	95% CI
T2WI	Mean	2	0.725	0.0748	0.602-0.827
	Mean	4	0.750	0.0664	0.629-0.848
	Mean	6	0.687	0.0736	0.562-0.795
	MPP	2	0.693	0.0669	0.568-0.800
	MPP	4	0.672	0.0723	0.547-0.782
	MPP	6	0.669	0.0745	0.544-0.780
	Skewness	0	0.728	0.0626	0.607-0.829
	Kurtosis	2	0.717	0.0644	0.595-0.820
	Kurtosis	4	0.678	0.0644	0.553-0.786
	Kurtosis	6	0.735	0.0637	0.614-0.835
	Entropy	0	0.745	0.0608	0.625-0.843
	Entropy	2	0.753	0.0595	0.633-0.849
	Entropy	4	0.793	0.0557	0.678-0.882
	Entropy	6	0.786	0.0576	0.669-0.876
T1WI	Kurtosis	0	0.679	0.0662	0.555-0.787
	Kurtosis	2	0.741	0.0635	0.620-0.840
	Kurtosis	4	0.745	0.0625	0.625-0.843
	Kurtosis	6	0.732	0.063	0.611-0.832
	Entropy	0	0.649	0.068	0.524-0.761
CE-T1WI	Mean	2	0.804	0.0588	0.690-0.891
	Mean	4	0.804	0.0578	0.690-0.891
	Mean	6	0.809	0.0573	0.695-0.894
	SD	2	0.662	0.0696	0.537-0.772
	MPP	2	0.739	0.0677	0.619-0.838
	MPP	4	0.776	0.0621	0.659-0.868
	MPP	6	0.785	0.0613	0.668-0.875
	Kurtosis	2	0.796	0.0535	0.681-0.883
	Kurtosis	4	0.817	0.0528	0.705-0.900
	Kurtosis	6	0.726	0.0608	0.606-0.827
	Skewness	6	0.678	0.0669	0.554-0.785
	Entropy	6	0.669	0.067	0.546-0.778

AUC = area under the receiver operating characteristic curve; CE-T1WI = contrast-enhanced T1-weighted image; CI = confidence interval; MPP = mean positive pixel; SD = standard deviation; SSF = special scale factor; T1WI = T1-weighted image; T2WI = T2-weighted image

Table 6. Diagnostic Performance of MR Texture Parameters from DWI and ADC for Differentiating Benign and Malignant Soft Tissue Tumors

Sequence	Texture parameter	SSF	AUC	Standard error	95% CI
DWI	Mean	0	0.674	0.0653	0.550-0.783
	Mean	2	0.721	0.0653	0.599-0.823
	Mean	4	0.700	0.0665	0.577-0.805
	Mean	6	0.641	0.0688	0.516-0.754
	SD	0	0.686	0.0677	0.562-0.793
	SD	4	0.653	0.0688	0.527-0.764
	SD	6	0.735	0.0634	0.614-0.835
	MPP	0	0.674	0.0653	0.550-0.783
	Skewness	6	0.665	0.0661	0.541-0.774
	Kurtosis	0	0.688	0.0644	0.565-0.794
	Kurtosis	2	0.795	0.0528	0.681-0.883
	Kurtosis	4	0.774	0.0572	0.657-0.866
	Kurtosis	6	0.716	0.0649	0.594-0.818
	Entropy	0	0.789	0.0535	0.674-0.878
	Entropy	2	0.774	0.0555	0.658-0.866
	Entropy	4	0.783	0.0547	0.668-0.873
	Entropy	6	0.784	0.0545	0.668-0.874
ADC	Mean	0	0.691	0.0658	0.568-0.796
	Mean	2	0.825	0.055	0.715-0.906
	Mean	4	0.846	0.0522	0.739-0.921
	Mean	6	0.852	0.0485	0.746-0.926
	SD	0	0.703	0.0674	0.580-0.807
	SD	4	0.653	0.0712	0.528-0.763
	SD	6	0.676	0.069	0.552-0.784
	MPP	0	0.691	0.0658	0.568-0.796
	MPP	4	0.713	0.0677	0.591-0.815
	MPP	6	0.751	0.0647	0.632-0.847
	Skewness	0	0.754	0.0594	0.635-0.850
	Skewness	4	0.649	0.068	0.525-0.760
	Skewness	6	0.678	0.0666	0.555-0.786
	Kurtosis	0	0.730	0.0629	0.610-0.830
	Kurtosis	2	0.730	0.0623	0.609-0.830
	Kurtosis	4	0.669	0.0678	0.545-0.777
	Kurtosis	6	0.684	0.0646	0.561-0.791
	Entropy	0	0.785	0.0542	0.669-0.875
	Entropy	2	0.781	0.0546	0.666-0.872
	Entropy	4	0.787	0.054	0.671-0.876
	Entropy	6	0.785	0.0542	0.669-0.875

ADC = apparent diffusion coefficient; AUC = area under the receiver operating characteristic curve; CI = confidence interval; DWI = diffusion-weighted image; MPP = mean positive pixel; SD = standard deviation; SSF = special scale factor

difference between benign and malignant myxoid soft-tissue tumors in kurtosis of ADC, but not in mean or SD of ADC (11). However, mean and SD as well as kurtosis showed significant differences in this study, perhaps because very few myxoid tumors were included in this study.

ADC is a key parameter for quantitative evaluation of DWI, but qualitative analysis of DWI with low and high b values is also useful, because DWI with high b value is not an inverted image of the ADC and has different information. Not all areas with low ADC values are highly cellular and may be fatty components or T2-blackouts caused by hematoma (26, 27). In other words, DWI and ADC play a complementary role. However, the MR texture parameters which differed in benign and malignant soft-tissue tumors in this study were almost identical in DWI and ADC. There was no significant difference between the diagnostic performances of DWI and ADC texture parameters, perhaps because only the first-order features from histogram analysis were used. Perhaps other information might be obtained from higher-dimensional textural analysis, but the information available only on DWI may not actually have helped distinguish between malignant and benign tumors.

There have been no reports about textural analysis of CE-T1WI and image filters for soft-tissue tumors. Most of the mean CE-T1WI, MPP of CE-T1WI, and kurtosis on CE-T1WI showed significant differences between malignancy and benign tumors in this study. This result may reflect the increased neovascularity and intratumoral heterogeneity of malignant tumors. For unfiltered images, none of the MR textural features potentially affected by differences in gain factors, including mean, SD, and MPP on T1WI, T2WI, and CE-T1WI, were significantly different between benign and malignant tumors in this study. However, for filtered images, some of those features showed significant differences between benign and malignant tumors, perhaps because the difference in signals by techniques was corrected by reducing noise (20). In other words, we think that the Laplacian of Gaussian filter provides additional normalization in a different way than using muscle signals does. There was no significant difference in diagnostic performance according to different filter sizes.

Our study has several limitations. There might have been selection bias, because this was a retrospective study. However, we recruited consecutive patients who satisfied the inclusion criteria in order to avoid selection bias. Small tumors were excluded because there were too few pixels to allow statistical significance. External validation with external data could not be done, because we had too few cases. The textural features obtained from the ROI measured in one slice of the tumor may not reflect the characteristics of the entire tumor and may thus act as a bias. Qualitative analysis using morphological features on conventional MR images could not be done. Only a few types of features were analyzed. In the future, research using higher-dimensional features and radiomics is needed.

In conclusion, accurate diagnosis could be obtained using MR textural analysis with DWI and CE-T1WI to differentiate benign from malignant soft-tissue tumors. Mean ADC on a 6-mm coarse filter was an independent factor that strongly suggested malignancy with a single MR feature.

REFERENCES

1. World Health Organization. Classification of tumours. In Fletcher CDM, Unni KK, Mertens F, eds. Pathology and genetics of tumors of soft tissue. Lyon: IARC Press; 2002:12-224
2. Surov A, Nagata S, Razek AA, Tirumani SH, Wienke A, Kahn T. Comparison of ADC values in different malignancies of the skeletal musculature: a multicentric analysis. Skeletal Radiol 2015;44:995-1000
3. Razek A, Nada N, Ghaniem M, Elkhamary S. Assessment of soft tissue tumours of the extremities with diffusion echoplanar MR imaging. Radiol Med 2012;117:96-101
4. Ahlawat S, Fritz J, Morris CD, Fayad LM. Magnetic resonance imaging biomarkers in musculoskeletal soft tissue tumors: review of conventional features and focus on nonmorphologic imaging. J Magn Reson Imaging 2019;50:11-27
5. Kransdorf MJ, Murphey MD. Imaging of soft-tissue tumors. 3rd ed. Philadelphia: Lippincott Williams & Wilkins (LWW), 2013
6. Chung WJ, Chung HW, Shin MJ, et al. MRI to differentiate benign from malignant soft-tissue tumours of the extremities: a simplified systematic imaging approach using depth, size and heterogeneity of signal intensity. Br J Radiol 2012;85:e831-836
7. Gruber L, Loizides A, Luger AK, et al. Soft-tissue tumor contrast enhancement patterns: diagnostic value and comparison between ultrasound and MRI. AJR Am J Roentgenol 2017;208:393-401
8. Lee SY, Jee WH, Jung JY, et al. Differentiation of malignant from benign soft tissue tumours: use of additive qualitative and quantitative diffusion-weighted MR imaging to standard MR imaging at 3.0 T. Eur Radiol 2016;26:743-754
9. Choi YJ, Lee IS, Song YS, Kim JI, Choi KU, Song JW.

Diagnostic performance of diffusion-weighted (DWI) and dynamic contrast-enhanced (DCE) MRI for the differentiation of benign from malignant soft-tissue tumors. J Magn Reson Imaging 2019;50:798-809
10. Lee KR, Ko SY, Choi GM. Quantitative T2 mapping of articular cartilage of the glenohumeral joint at 3.0T in rotator cuff disease patients: the evaluation of degenerative change of cartilage. Investig Magn Reson Imaging 2019;23:228-240
11. Kim HS, Kim JH, Yoon YC, Choe BK. Tumor spatial heterogeneity in myxoid-containing soft tissue using texture analysis of diffusion-weighted MRI. PLoS One 2017;12:e0181339
12. Makanyanga J, Ganeshan B, Rodriguez-Justo M, et al. MRI texture analysis (MRTA) of T2-weighted images in Crohn's disease may provide information on histological and MRI disease activity in patients undergoing ileal resection. Eur Radiol 2017;27:589-597
13. Patel N, Henry A, Scarsbrook A. The value of MR textural analysis in prostate cancer. Clin Radiol 2019;74:876-885
14. Qiu Q, Duan J, Duan Z, et al. Reproducibility and non-redundancy of radiomic features extracted from arterial phase CT scans in hepatocellular carcinoma patients: impact of tumor segmentation variability. Quant Imaging Med Surg 2019;9:453-464
15. Corino VDA, Montin E, Messina A, et al. Radiomic analysis of soft tissues sarcomas can distinguish intermediate from high-grade lesions. J Magn Reson Imaging 2018;47:829-840
16. Parikh J, Selmi M, Charles-Edwards G, et al. Changes in primary breast cancer heterogeneity may augment midtreatment MR imaging assessment of response to neoadjuvant chemotherapy. Radiology 2014;272:100-112
17. Wang H, Zhang J, Bao S, et al. Preoperative MRI-based radiomic machine-learning nomogram may accurately distinguish between benign and malignant soft-tissue lesions: a two-center study. J Magn Reson Imaging 2020;52:873-882
18. Wang H, Nie P, Wang Y, et al. Radiomics nomogram for differentiating between benign and malignant soft-tissue masses of the extremities. J Magn Reson Imaging 2020;51:155-163
19. Lim HK, Jee WH, Jung JY, et al. Intravoxel incoherent motion diffusion-weighted MR imaging for differentiation of benign and malignant musculoskeletal tumours at 3 T. Br J Radiol 2018;91:20170636
20. Lubner MG, Smith AD, Sandrasegaran K, Sahani DV, Pickhardt PJ. CT Texture analysis: definitions, applications, biologic correlates, and challenges. Radiographics 2017;37:1483-1503
21. De Cecco CN, Ganeshan B, Ciolina M, et al. Texture analysis as imaging biomarker of tumoral response to neoadjuvant chemoradiotherapy in rectal cancer patients studied with 3-T magnetic resonance. Invest Radiol 2015;50:239-245
22. Peng H, Long F, Ding C. Feature selection based on mutual information: criteria of max-dependency, max-relevance, and min-redundancy. IEEE Trans Pattern Anal Mach Intell 2005;27:1226-1238
23. Youden WJ. Index for rating diagnostic tests. Cancer 1950;3:32-35
24. DeLong ER, DeLong DM, Clarke-Pearson DL. Comparing the areas under two or more correlated receiver operating characteristic curves: a nonparametric approach. Biometrics 1988;44:837-845
25. Berenguer R, Pastor-Juan MDR, Canales-Vazquez J, et al. Radiomics of CT features may be nonreproducible and redundant: influence of CT acquisition parameters. Radiology 2018;288:407-415
26. Hiwatashi A, Kinoshita T, Moritani T, et al. Hypointensity on diffusion-weighted MRI of the brain related to T2 shortening and susceptibility effects. AJR Am J Roentgenol 2003;181:1705-1709
27. Maldjian JA, Listerud J, Moonis G, Siddiqi F. Computing diffusion rates in T2-dark hematomas and areas of low T2 signal. AJNR Am J Neuroradiol 2001;22:112-118